

All-fiber optical sensor of electrical current with a SPUN fiber sensing element

V. P. Gubin, V. A. Isaev, S. K. Morshnev, A. I. Sazonov, N. I. Starostin, Yu. K. Chamorovsky, A. I. Oussov, S.Yu. Otrokhov

The Institute of Radio Engineering and Electronics
Russian of Academy of Sciences, Moscow region, Russia

ABSTRACT

A fiber optic current sensor (FOCS) using the Faraday effect in a fiber coil is presented. The current sensor is realized on the base of the all-fiber low-coherent reflection interferometer. An Erbium-doped fiber superfluorescent radiation source and a sensing SPUN hi-bi fiber coil are applied in the interferometer. The detectivity of the sensor is about 70 mA/ $\sqrt{\text{Hz}}$, the scale factor error is about $\pm 0.5\%$, the range of measured currents is 0.1A – 3000 A, and the bandwidth is up to 10 kHz. Some physical and technical sources of the FOCS scale factor errors are studied. It is shown that the normalized optical scale factor of the FOCS is virtually independent of the SPUN fiber length for a given coil diameter. The evaluative relation for the FOCS scale factor error owing to the spectrum instability of light wideband source is given.

Key words: optical current sensor, Faraday effect, spun fiber

1. INTRODUCTION

Interferometric fiber optic sensors are the most accurate measurement instrumentation, and this fact stimulates their research and development. One of the most promising and attractive sensors is a fiber optic current sensor (FOCS) using the Faraday effect in fused silica fiber wound around a conductor with electric current.

These FOCSs have good field-performance data, such as inherent isolation from high voltage power circuit, simplicity of service and low size and weight. Furthermore, they have fast response, and their output signal is compatible with computer networks. Such FOCS can be used in high-voltage and low-voltage electric power industry systems as the base for the replacement of current transformers, for the control of leakage currents, as well as reference current standards.

An interferometric method for detecting the Faraday effect is realized in the following way. A magnetic field of measured current induces a phase shift between the circularly polarized fiber modes (magneto-optic Faraday phase shift)¹. This shift is recorded by a method of low-coherent interferometry, that allows one to realize high measurement accuracy of physical magnitudes. For this purpose, a superluminescent diode (SLD) or a superfluorescent erbium-doped fiber source (SFS) can be used as a wideband radiation source. At present, the SFS meets the requirement of high accuracy in the best way².

In particular, it has higher output power and higher radiation spectrum stability as compared with the SLD. The operated wavelength of the SFS is in the range of 1.55 μm , which is widely used for optical communication.

At present, the achievement of the accurate FOCS scale factor in the widely temperature range remains the most important problem. The main task is the reduction of possible linear birefringence in a sensing fiber coil³, which does not only influence the scale factor value, but also leads to the appearance of unwanted sensitivity to outside magnetic fields non-connected with the measured current. Different methods have been proposed to reduce the linear birefringence. Among them are the following: (i) thermal annealing of sensing fiber¹; (ii) twisting of low-birefringence silica fiber⁴; (iii) using SPUN fiber⁵. The best results are achieved with the use of thermally annealed fiber. However, the use of SPUN fiber for the sensing FOCS coil has some potential technological advantages over the annealed sensing fiber coil.

This paper is devoted to the experimental and theoretical research of some effects that produce the scale factor error in an interferometric reflection FOCS. In this FOCS, the erbium-doped fiber source and the sensing SPUN fiber coil are employed. The prototype FOCS has the accuracy characteristics close to those that are necessary for the application in electrical power industry.

2. EXPERIMENTAL SET-UP

The optical scheme FOCS is an all-fiber reflection linear interferometer (Fig.1) with two orthogonal polarization light waves⁶. If the electrical current in the conductor 12 is absent, these light waves have zero difference of optical paths. The main components of interferometer are radiation source 1, directional coupler 3 with photodiode 2 at output, polarizer 5, birefringence modulator 7, connective polarization maintaining fiber line 8, phase quarter-wave plate 9, sensing fiber coil 10 with mirror 11. The fusion splices 4, 6 are used for connecting the FOCS fiber elements. The fusion splices 6 are fulfilled with a 45° angular offset in the core orientation. The electronic signal processing scheme consists of a phase detector 13 and a reference oscillator of sinusoidal voltage 14. The phase detector provides an output analog signal proportional to the measured current. The digital output is fulfilled on the base of an analog-digital converter 15, which is connected to a computer 16.

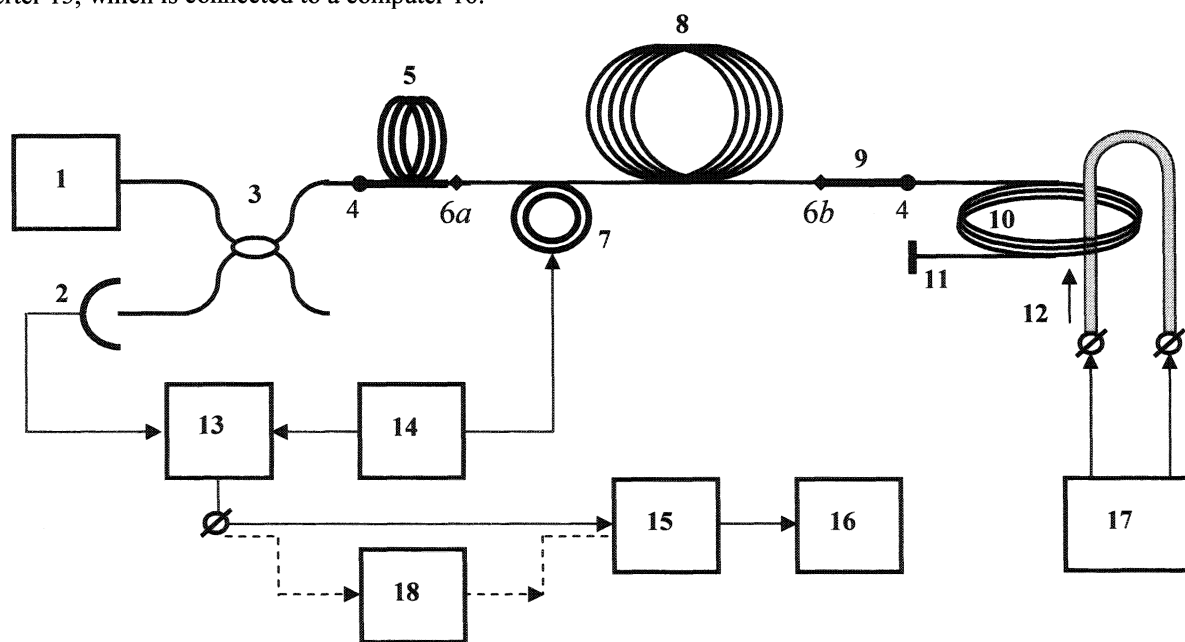


Figure 1. The FOCS setup (17 - current supply, 18 - spectrum analyzer)

The sensor operates in the following way. Two orthogonal linear polarized fiber modes (x and y modes) with equal intensities are created on input fiber birefringence modulator (splice $6a$). These fiber modes pass through a fiber line. The quarter-wave fiber phase plate transforms linear orthogonal polarizations into the left- and right- polarized circular modes. Circular polarization light waves pass through the sensing coil in both directions and accumulate a non-reciprocal phase shift φ_F in proportion to the measured current. The rotation direction of the circular modes is reversed after the reflection from the mirror. As a result, these modes undergo conversion on the back passage of the fiber phase plate, i.e., x mode is transformed to y mode and vice versa. As a consequence all phase shifts in the interferometer output, except φ_F , will be compensated, and the light intensity on the photodiode will depend on φ_F in the following way:

$$P(\varphi_F) = \frac{1}{2} P_0 (1 + \cos \varphi_F), \quad \varphi_F = 4 V N I. \quad (1)$$

Here V is the Verdet constant of SPUN fiber, N is the number of fiber turns around a conductor with current I .

An erbium-doped fiber source used in the sensor had the output power of about 10 mW at a wavelength of 1.55 μm . The spectrum width of the fiber source was about 15 nm. A birefringence phase modulator was made of polarization

maintaining fiber (Panda type) wound around a piezoceramic cylinder with 32 mm in diameter. Modulator was placed at the beginning of the fiber line and operated at the resonant frequency of the cylinder $f_m = 40$ kHz, supporting necessary amplitude of dynamic phase shift between x and y modes⁶. The fiber line had a length of 900 m and was made of Panda type fiber with the h parameter $2 \cdot 10^{-5} \text{ m}^{-1}$. A phase quarter-wavelength plate was made of Panda type fiber with a polarization beat length about 4 mm. For this purpose, we applied a long Panda fiber. We aligned the birefringence axes of this fiber at 45° with respect to the axes of the PM connective fiber line. Measuring the depolarization of the output light, we checked an angle of 45° . After execution of the fusion splice 6b, we cleaved the long fiber at 1/4 of a beat length from the 45° splice⁷. Sensing coil was made out of 27 turns of SPUN hi-bi fiber (unspun beat length of about 20mm, a spin pitch of about 500 twist/m, a fiber diameter $125\mu\text{m}$) wound around the dielectric ring of a 160 mm diameter. The conductor with current was placed in the form of toroid winding around the dielectric ring. At the same time, each of 370 toroidal turns passed through the inner hole of the dielectric ring. This design supported the equivalent current through the coil plane exceeding the actual current by a factor of 370. Other designs of the sensing coils were also employed in the experiments.

3. EXPERIMENTAL RESULTS

Fig.2 shows the FOCS output voltage U_0 as a function of equivalent direct current I_0 passing through the fiber sensing coil (FOCS output characteristic). The largest measured current was equal to 3000 A. The current definition error was about 0.1 % at $I_0 > 10$ A.

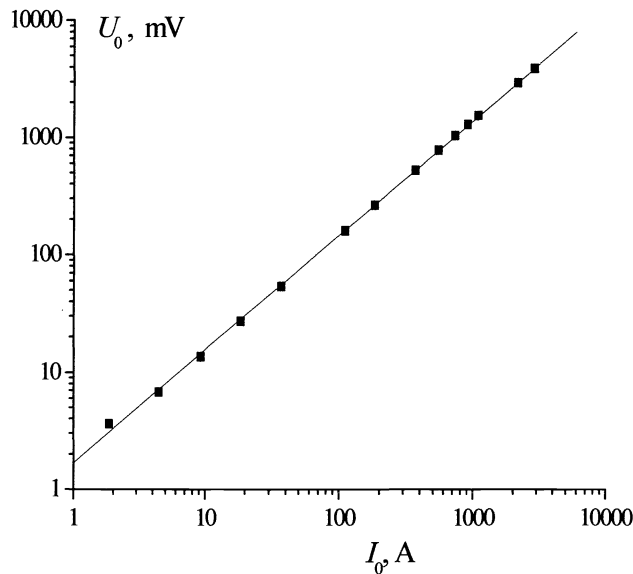


Figure 2. FOCS output characteristic

Fig.3 shows the FOCS output voltage $U_0(t)$ as a function of time for 2 hours at $I_0 = 1.85$ A (a) и 370 A (b), respectively. The records at the beginning and the end of the plot correspond to $I_0 = 0$. The bandwidth of the electronic processing scheme was equal $B = 1$ Hz. According to Fig. 3(b), the FOCS scale factor was $k_1 = \langle U_0 \rangle / I_0 = 6.4 \text{ mV/A}$, its instability was $\Delta U_0 / \langle U_0 \rangle = 0.1 \%$ (1σ) for 2 hours, where $\langle U_0 \rangle$ is an average value, ΔU_0 is standard deviation of the FOCS output voltage. According to Fig. 3(a), the FOCS detectivity was about $I_{\min} = 0.16 \text{ A}/\sqrt{\text{Hz}}$. It is necessary to note that this value was limited by the resolution of the electronic processing block, and the actual magnitude, caused by the radiation noise, was about $70 \text{ mA}/\sqrt{\text{Hz}}$. It is interesting to note that ΔU_0 in Fig. 3(b) at $I_0 \neq 0$ is determined by current fluctuations and is greater than I_{\min} .

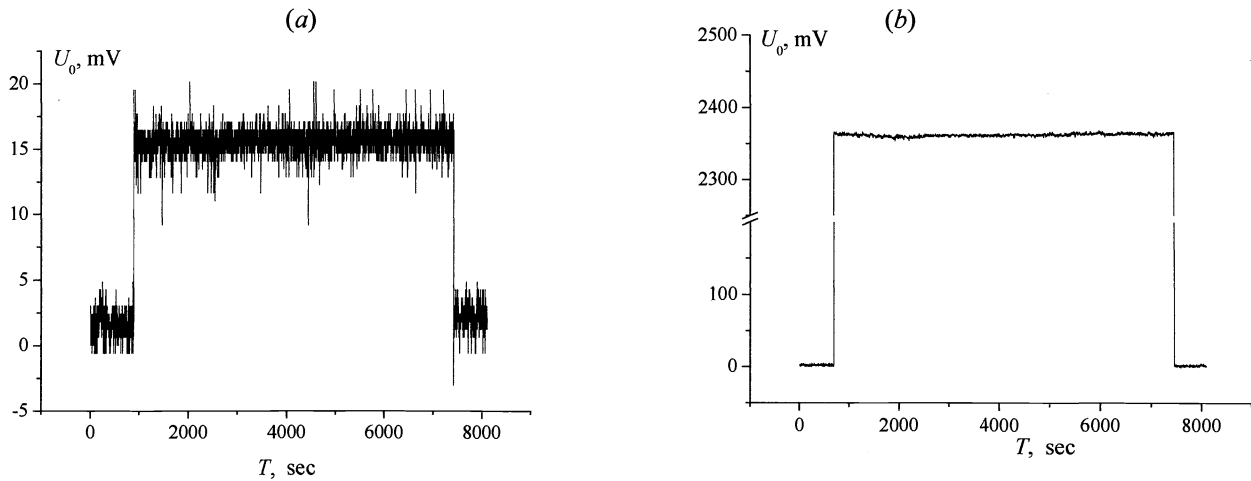


Figure 3. Long term stability of the FOCS output

Fig.4 shows the measurement results of the direct electrical current ($I_o=185A$) during 19 days. These measurements allow one to estimate the scale factor repeatability of the given FOCS. During the measurements the optical power on photodiode was checked and these data were normalised to some fixed power. The set-up was warmed up two hours before the measurements. The environment temperature varied from 10 to 18 °C from day to day. According to all available measurements, the error of optical scale factor was about $\pm 0.5\%$ (rms).

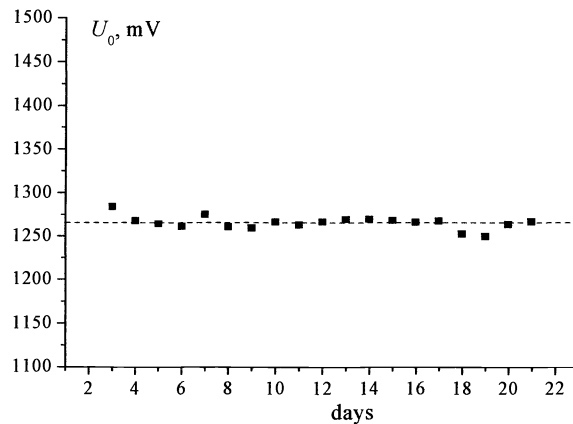


Figure 4. A repeatability of the FOCS output

An oscilloscope trace of the alternating current in a conductor recorded with the help of the FOCS (bandwidth of electronic processing block $B = 900$ Hz) is shown in Fig.5 (a). A 50 Hz power mains was the alternating current supply. During the experiment a separating step-down transformer was employed to connect the conductor to the power mains. From Fig.5 (a) we can see that the alternating current has some small symmetrical distortions on a half-cycle tip. The spectrum of the FOCS output signal for this case is shown in Fig.5 (b). The spectrum contains a number of odd harmonics with decreasing amplitudes. For comparison, Fig.5 (c) shows the spectrum of the voltage across the conductor lead terminals. This voltage determines the measured current. A satisfactory agreement is observed between Fig.5 (b) and Fig.5 (c). Some discrepancy at high frequencies can be explained by the conductor inductive impedance influencing in different ways on the lead terminals voltage and on the current through conductor.

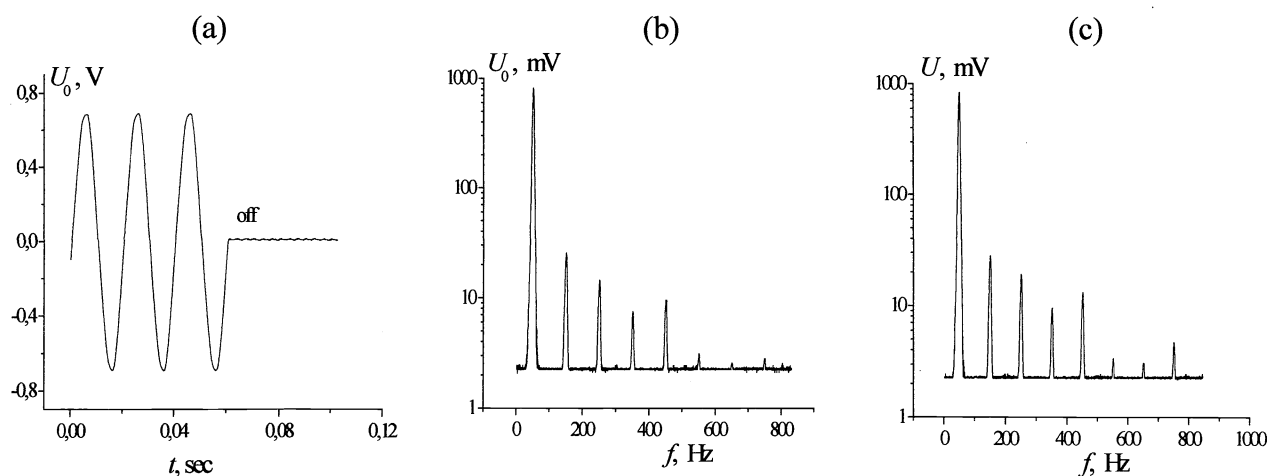


Figure 5. Power mains (50 Hz): (a) FOCS output oscilloscope trace, (b) FOCS output signal spectrum, (c) spectrum of voltage across conductor lead terminals

Fig.6 shows FOCS scale factor versus temperature of phase plate. We can see that all magnitudes of the scale factor are situated within 0.5 % interval over the temperature range 80 °C.

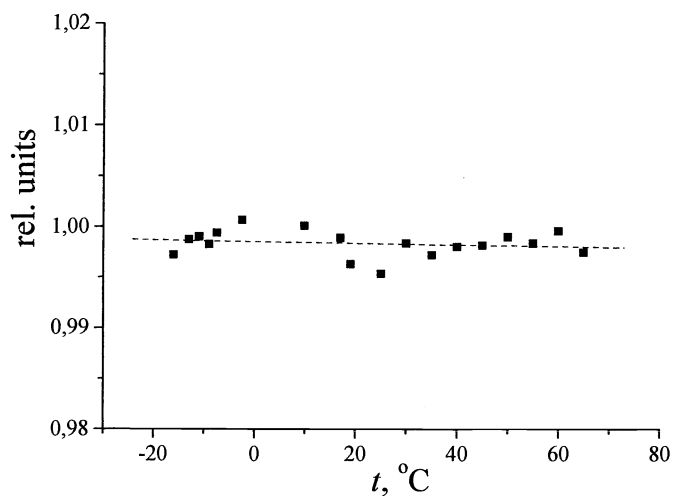


Figure 6. Effect of phase plate temperature on FOCS scale factor.

A developed model of the FOCS was used to study of the effects which determine the scale factor error due to the induced bend birefringence into SPUN fiber. The scale factor dependencies on the number of fiber turns N , the fiber length L and the diameter D of the sensing coil were studied. The study was fulfilled by the direct current $I_0 = 10$ A. The normalized scale factor value (or rather normalized sensitivity Q of the sensor) was expressed in mV/(A.turn).

Fig.7 shows $Q(L)$ measured for several D . The measurement error was less 5 % (it is to note that the data averaging was carried out at a low length). These functions have the following features: (i) In the mean, at constant diameter sensitivity does not depend on L (and consequently, N), with the exception of low L at $D = 20$ mm; (ii) at $D > 40$ mm Q nearly does not depend on D , but at smaller diameters Q is greatly degraded;

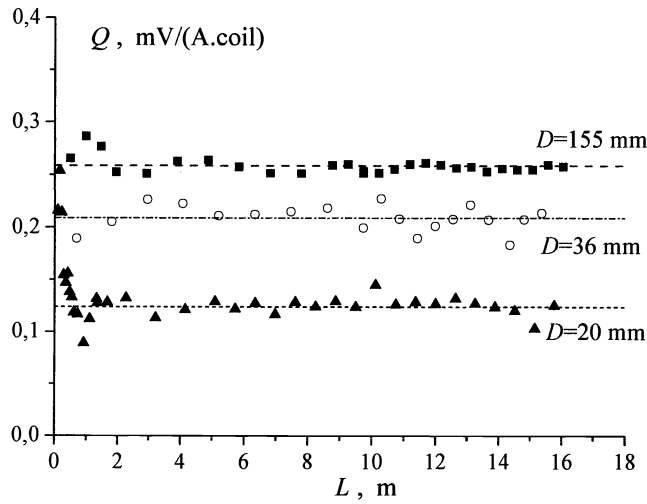


Figure 7. The normalized sensitivity of SPUN fiber at different coil diameter.

(iii) small sensitivity discrepancies from the average value are found at some fiber lengths. However, Q has high stability if the coil geometry is constant. The above-mentioned discrepancies exceed the measurement errors and occur at both the big and the small diameters. It is possible that they are caused by incidental perturbation actions on the fiber during the coil winding. Fig.8 shows $Q(D)$ measured for $L = 16$ m.

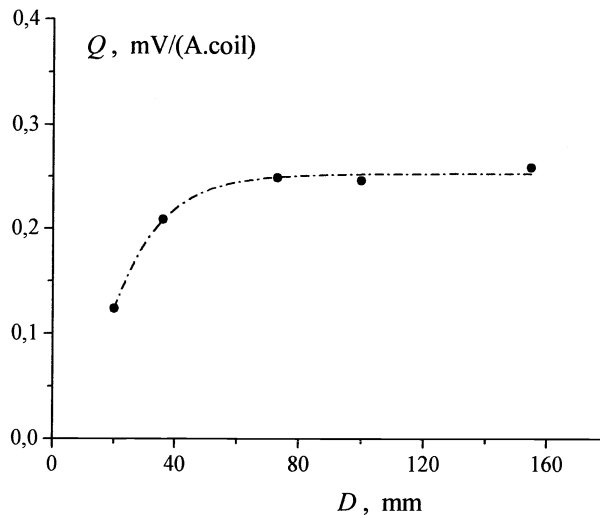


Figure 8. Normalized the FOCS sensitivity as a function of the coil diameter

4. DISCUSSION

The FOCS detectivity is limited by shot and excess noise of radiation. FOCS output may be expressed analogously to a fiber optic gyroscope⁸. The FOCS detectivity can be calculated for the first harmonic of the output as

$$I_{\min}(1\sigma) = \frac{1}{s} \frac{1+J_0}{J_1} \frac{1}{4NV} \left[B \left(\frac{e}{Pq} + \frac{\lambda_0^2}{2c\Delta\lambda} \right) \right]^{1/2} \quad (2)$$

where $s = P / (P + P_0) < 1$ is the FOCS output signal contrast determined as the ratio of the useful portion P to the whole light power on the photodiode (P_0 is a unwanted portion), q is a quantum photodiode response (in A/W), $J_0(\psi_m)$ and $J_1(\psi_m)$ are Bessel functions of first kind, ψ_m is a phase modulation amplitude, B is a bandwidth electronic processing scheme. The first summand in (2) corresponds to shot noise, the second one is excess noise.

An estimate of the FOCS detectivity for our FOCS gives $I_{\min} = 25 \text{ mA}/\sqrt{\text{Hz}}$. The following values of the FOCS parameters were used: $P = 100 \text{ } \mu\text{W}$, $s = 0.93$, $\psi_m = 1.17 \text{ rad}$, $J_0 = 0.69$, $J_1 = 0.49$, $N = 27$, $V = 0.71 \text{ } \mu\text{rad}/\text{A}^{10}$, $B = 1 \text{ Hz}$, $q = 0.7$, $\lambda_0 = 1.55 \text{ } \mu\text{m}$, $\Delta\lambda = 15 \text{ nm}$. The analysis shows that the FOCS detectivity is determined by the excess noise of wide-band radiation. One of the causes of the discrepancy between the calculated and measured values of I_{\min} can be the core composition of our SPUN fiber⁹. The sensor zero shift (when the electric current passing the fiber sensing coil is zero) is a principal origin of error at low currents. It causes a zero drift of the output signal. In the experiments (during 19 days) the zero drift was characterised by the average value and the standard deviation of the equivalent current 28mA and 310 mA, respectively. For $I = 185 \text{ A}$ the given drift yielded a contribution of about 0.17 % in the measurement error. To our knowledge, the main origin of the zero shift is a parasitic amplitude modulation in the birefringence phase modulator. This parasitic signal is caused by the bend loss modulation and detected on the phase modulation frequency. The phase of parasitic modulation signal is shifted on 90 degrees with respect to a useful one. Therefore, the actual zero drift was caused by a phase mismatch of reference signal relative of the quadrature tuning to the parasitic modulation signal. This mismatch was due to the instability of the resonance frequency of the fiber modulator.

Theoretically the FOCS bandwidth may be very large. It is limited by the propagation time of the light wave through the fiber sensing coil. From the practical standpoint the bandwidth must be chosen less than the phase modulation frequency so as to avoid the aliasing spectra problem. In our FOCS, the maximum bandwidth is about 10 kHz.

4.1. Source spectrum influence on scale factor of theFOCS

Analogously to the fiber optic gyroscope, the scale factor of the low coherence current sensor depends on the spectrum shape and its location within the frequency domain⁸. However, in the gyroscope a Sagnac phase shift is proportional to the light frequency ν , while, in the current sensor, a Faraday phase shift is proportional to ν^2 (the Verdet constant has dependence $V = k_\nu \nu^2$, where k_ν is a constant¹⁰). In order to estimate the influence of the spectrum on the FOCS scale factor, we consider the output sensor signal on the light component $P(\nu)$ at the narrow frequency band $d\nu$ and then summarize within the source spectral range ($\nu_1 \dots \nu_2$). Assuming that the detection is carried out on the first harmonic component of the phase modulated output signal, the following equation for the photodiode current can be written for low φ_F at the frequency ν :

$$di_{d1} \approx P(\nu) J_1(\psi_m) \eta \varphi_F(\nu) d\nu = k I P(\nu) \nu^2 d\nu \quad (3)$$

where φ_F is determined by (1), η is parameter taking into account the sensitivity reduction owing to the imperfection of the FOCS fiber elements, $k = 8 J_1(\psi_m) N k_\nu \eta$. The whole photodiode current is given by

$$i_{d1} = k I \int_{\nu_1}^{\nu_2} P(\nu) \nu^2 d\nu$$

or, passing to the decomposition of the spectrum into n intervals with wide $\Delta\nu$

$$i_{d1} = k I \sum_{i=1}^n P(\nu_i) \nu_i^2 = k I P \langle \nu^2 \rangle \quad (4)$$

where

$$\langle \nu^2 \rangle = \left[\sum_{i=1}^n P(\nu_i) \nu_i^2 \right] / \left[\sum_{i=1}^n P(\nu_i) \right], \quad P = \sum_{i=1}^n P(\nu_i) \quad (5)$$

Here, $\langle \nu^2 \rangle$ is the average weighted square of the spectrum frequency, P average power of light. Taking in account that at $\Delta\nu \ll \nu$ we have $\Delta\nu/\nu \cong \Delta\lambda/\lambda$, instead of (4) and (5) we can write

$$i_{d1} = k I P c^2 / \langle \lambda^2 \rangle \quad (6)$$

$$\langle \lambda^2 \rangle = \left[\sum_{i=1}^n \lambda_i^2 P(\lambda_i) \right] / \left[\sum_{i=1}^n P(\lambda_i) \right], \quad P = \sum_{i=1}^n P(\lambda_i) \quad (7)$$

where $\langle \lambda^2 \rangle$ is the average weighted square of the wavelength of the radiation source. Thus, the scale factor of the current sensor $k_I = i_{d1} / I$ may be expressed as

$$k_I = 8 J_1(\psi_m) N k_V \eta P c^2 / \langle \lambda^2 \rangle \quad (8)$$

4.2 Reduction methods of scale factor error

From (8) it can be concluded that the main parameters which cause an error at the detection first harmonic component of modulated output are ψ_m , k_V , P , η and $\langle \lambda^2 \rangle$.

We shall estimate the error due to $\langle \lambda^2 \rangle$ instability for two sources –the SLD and the erbium fiber source. The analysis of the actual spectra of the erbium source showed that one can use λ_0^2 instead of $\langle \lambda^2 \rangle$. Here, λ_0 is the average weighted wavelength of the radiation source and it is given by ²

$$\lambda_0 = \left[\sum_{i=1}^n \lambda_i P(\lambda_i) \right] / \left[\sum_{i=1}^n P(\lambda_i) \right] \quad (9)$$

It can be shown that the scale factor error $\Delta k_I / k_I \cong 2 \Delta \lambda_0 / \lambda_0$ for low shifts. Assuming that for the SLD the temperature instability of λ_0 is about $\Delta \lambda_0 / \lambda_0 \approx -400$ ppm/°C we find that the error is 8 % for 100 °C temperature range. This value sufficiently exceeds reasonable error in the power industry applications (± 0.2 %). Under such conditions, the erbium fiber source having the temperature wavelength instability less than 5 ppm/°C ² allows to reduce the error as high as ± 0.1 %.

To reduce the instability influence of the phase modulation amplitude ψ_m and the source average power P , one can apply a processing signal scheme calculating harmonic components ratio of the sensor output ⁸. Using the ratio of the first and the second harmonic one can reduce the influence of the power variations and at the same time preserve an information about the measured current. Using of the ratio of the second and the fourth harmonic one can reduce the influence of variations of ψ_m because this ratio does not depend on the measured current but depend on the phase modulation amplitude. Preliminary estimates show that this method allows one to reduce the scale factor errors due to P and ψ_m variations to 0.05 % in a broad temperature range. The modulation frequency in the experiments was tuned to the resonance of the piezoceramic cylinder, and the modulation voltage at the piezoceramic cylinder was kept constant, however, the magnitude of ψ_m is not directly measured. In our opinion, a variation of ψ_m due to the instability resonance frequency of the fiber phase modulator was the main source of the scale factor error of the our current sensor.

The most complex problem is physical and technical phenomena that affect the coefficients k_V and η . Among the main unwanted effects one can note the followings: instability of bend linear birefringence within the sensing coil ³, thermal sensitivity of the phase quarter-wave plate ⁷ and temperature dependence SPUN fiber parameters ⁵. Various ways to reduce the influence of these effects was proposed in the above cited papers. Our experimental study showed that the phase quarter-wave plate made of Panda type fiber has a temperature coefficient (see Fig.6) near to one for the elliptical core fiber retarder. This result contrasts to the well-known results ¹¹. In accordance, with this paper, the temperature birefringence dependence of PM fibers with stress-induced birefringence is about an order of magnitude greater than that of the elliptical core fiber. The origin of such a behavior of our phase quarter-wave plate is not interpreted.

The dependence of the normalized FOCS sensitivity on the coil diameter (see Fig.7) may be explained by the bend effect that induces the linear birefringence in the fiber coil. Our theoretical analysis that will be published elsewhere shows that the sensitivity reduction at $D < 70$ mm for the Spun fiber coil is caused first of all by the bend-induced birefringence. It is interesting to note that, in accordance with this analysis, the sensitivity reduction occurs when the inherent linear birefringence of the Spun fiber significantly exceeds the bend-induced linear birefringence.

5. CONCLUSION

The Fiber optic current sensor (FOCS) employing the Faraday effect in a fiber coil is presented. The current sensor is realized on the base of an all-fiber low-coherent reflection interferometer. The erbium-doped fiber source of the radiation and the SPUN fiber sensing coil are applied in the interferometer. The prototype current sensor has the following characteristics: detectivity about $70 \text{ mA}/\sqrt{\text{Hz}}$, operating current range up to 3000 A, bandwidth up to 10 kHz, scale factor error about $\pm 0.5 \%$. It is experimentally shown that the FOCS normalized optical scale factor does not practically depend on the SPUN fiber length at the given coil diameter. At some fiber lengths a small discrepancy of scale factor from the average value are found. They are apparently concerned with incidental perturbation actions on fiber caused by the coil winding process. It is pointed that one of the causes of a sensor zero shift is a parasitic amplitude modulation in the birefringence phase modulator. This parasitic signal is caused by the bend loss modulation and detected at the phase modulation frequency. A relation is obtained to estimate the influence of the wideband source spectrum instability on the FOCS scale factor.

ACKNOWLEDGEMENT

The authors would like to thank V.P. Gapontsev and I.E. Samartsev for supporting of this work.

REFERENCES

1. K. Bohnert., P. Gabus, J. Nehring, H. Brändle, "Temperature and vibration insensitive fiber-optic current sensor", *J. Lightwave Technol.*, **20**, pp. 267-276, 2002.
2. P. F. Wysotski, M.J. Dignonnet, B.Y. Kim, H.J. Shaw, "Characteristics of Erbium-Doped Superfluorescent Fiber Sources for Interferometric Sensor Applications", *J. of Lightwave Technol.*, **12**, pp. 550-567, 1994.
3. S. X. Short, J.U. De Arruda, A. A. Tselikov, J. N. Blake, "Elimination of Birefringence Induced Scale Factor Errors in the In-Line Sagnac Interferometer Current Sensor", *J. of Lightwave Technol.*, **16**, pp. 1844 -1850, 1998.
4. M. Takahashi et al., " Optical Current Transformer for Gas Insulated Switchgear Using Silica Optical Fiber", *IEEE Trans. On Power Delivery*, **12**, pp. 1422-1427, 1997.
5. R. I. Laming , D. N. Payne, "Electric current sensors employing spun highly birefringent optical fibers", *J. of Lightwave Technol.*, **7**, pp. 2084-2094, 1989.
6. G. Frosio, R. Dandliker, "Reciprocal reflection interferometer for a fiber-optic Faraday current sensor", *Applied Optics*, **33**, pp. 6111-6122, 1994.
7. S. X. Short, A. A. Tselikov, J.U. de Arruda, J. N. Blake, "Imperfect quarter-waveplate compensation in Sagnac interferometer-type current sensors", *J. Lightwave Technol.*, **16**, pp. 1212-1219, 1998.
8. R. P. Moeller, W.K. Burns, N. J. Frigo "Open-loop output and scale factor stability in a fiber-optic gyroscope", *J. of Lightwave Technol.*, **7**, pp. 262-269, 1989.
9. V. I. Aksenov et al., "The Faraday Effect in Quartz Optical Fibers" *Journal of Communications Technology and Electronics*, **47**, pp. 919-925, 2002.
10. A. H. Rose, S. M. Etzel, C. M. Wang "Verdet constant dispersion in annealed optical fiber current sensors", *J. Lightwave Technol.*, **15**, pp. 803-807, 1997.
11. F. Zhang and J. W. Y. Lit "Temperature and strain sensitivity measurements of high-birefringent polarization-maintaining fibers", *Applied Optics*, **32**, pp. 2213-2217, 1993.